# Resource Management in Multicloud IoT Radio Access Network

Muhammad Awais, Ashfaq Ahmed, Syed Azhar Ali, Muhammad Naeem, Waleed Ejaz, *Senior Member, IEEE*, and Alagan Anpalagan

***Abstract*—Cloud radio access network (CRAN) is a promising approach to provide ubiquitous and on demand access to future Internet of Things (IoT) networks. The existing CRANs assume a single cloud which suffers from computational complexity and signaling latency to support massive number of IoT devices in large scale network deployments. This paper focuses on the scheduling of IoT devices in a multicloud IoT network scenario. This paper considers the downlink of an IoT network consisting of multiple clouds, each coordinates a cluster of several base stations (BSs) allowing joint signal processing. The transmit frame of each BS is composed of several resource blocks (RBs). The multiple clouds are linked to the central cloud which performs scheduling of IoT devices and synchronization of transmit frames. The work models the IoT devices to RBs assignment problem considering the intercloud and intracloud interference. The optimization problem maximizes the overall network utilization under practical network constraints. Further, this paper also proposes a low complexity heuristic algorithm to solve the constraint resource allocation problem in linear time. Complexity analysis of proposed algorithm is carried out and simulations results for a number of IoT network scenarios demonstrate that proposed solution is numerically accurate and performs close to the optimal solution.**

***Index Terms*—Greedy algorithm, Internet of Things (IoT), radio access networks, resource allocation.**

## I. Introduction

Internet of Things (IoT) refers to a set of smart, uniquely identifiable computing devices connected to the Internet. The massive deployment of IoT devices causes several challenges, including increased volume, high data rates, spectrum scarcity, energy efficiency, and strict latency requirements. Integration of IoT systems in existing and 5G networks is the key to address these challenges. A combination of 5G and industrial IoT (IIoT) is now becoming an emerging paradigm for connectivity and data transfer. Applications of 5G assisted IIoT includes, but not limited to, wireless sensor networks [1], [2], concurrent data collections [3], device-to-device and data aggregation [4], monitoring solution for advanced predictive maintenance applications [5], cyber-physical systems [6], energy management [7], machine-to-machine communications [8], ecosystem [9], agriculture [10], smart cities [11], healthcare [12], and video streaming [13], etc.

The practical large scale IoT networks consist of hundreds to thousands of IoT devices, including the cell phones, the buildings, the traffic signals, the vehicles, etc. Therefore, an efficient radio resource management is of utmost importance to ensure smooth functioning of network with low latency and high throughput [14].

Cloud radio access network (CRAN) is a promising network architecture to meet the massive increase in data traffic for future IoT deployment. The key concept behind CRAN is that it breaks down the conventional base station (BS) in to a baseband unit (BBU) and a remote radio head (RRH). The BBUs perform the intensive base band signal processing activities whereas, RRHs are light computational elements which perform tasks, such as signal modulation and amplification, etc. The CRAN centralizes the computation resources of several BBUs in to a central location called the cloud data center or baseband resource pool (BRP). The RRHs are spread to cover the required geographical area. A high speed communication network connects the RRHs with the BBUs. The BRP consists of several software defined virtual computing resources which are dynamically shared by all RRHs in the network. Centralization of computing resources allows several techniques, including coordinated multipoint transmission and joint beamforming. CRAN offers a number of advantages, such as effective scheduling of users (devices) and resource allocation, increased network utilization, energy efficiency, and smaller interference through interbase station coordination.

The CRAN scenarios can be classified as single-CRAN or multi-CRAN. In a single-CRAN, there is only one cloud that centralizes the activities of its connected BSs. The central cloud is responsible for scheduling policy, power control, and synchronization of transmit frames across the network. The resource allocation decisions are made by the cloud according to some predefined performance optimization objective. The RRHs are connected to the cloud through high speed backhaul links. This allows coordination through joint signal processing between the connected BSs. As a result, low interference and high energy efficiency is achieved. While single-CRAN is

Manuscript received August 15, 2018; revised October 4, 2018 and October 16, 2018; accepted October 22, 2018. Date of publication October 29, 2018; date of current version May 8, 2019. *(Corresponding author: Waleed Ejaz.)*

M. Awais, A. Ahmed, and M. Naeem are with the Department of Electrical and Computer Engineering, COMSATS University Islamabad (Wah Campus), Wah Cantonment 47040, Pakistan.

S. A. Ali is with the Department of Electronic Engineering, University of Engineering and Technology at Taxila, Taxila 47050, Pakistan.

W. Ejaz is with the Department of Applied Science and Engineering, Thompson Rivers University, Kamloops, BC V2C 0C8, Canada (e-mail: wejaz@tru.ca).

A. Anpalagan is with the Department of Electrical and Computer Engineering, Ryerson University, Toronto, ON M5B 2K3, Canada (e-mail: alagan@ee.ryerson.ca).

Digital Object Identifier 10.1109/JIOT.2018.2878511

considered in majority of existing works on resource allocation, it can suffer from latency, poor energy efficiency, and connectivity problems in massive IoT networks, especially with real time communication requirements. Moreover, single-CRANs treat the intercloud interference as background noise while assuming perfect CSI available at the cloud, which is not often practical [15].

This paper considers a multi-CRAN which is more practical scenario for dense multicell IoT networks, with hundreds of IoT devices spread over large geographical area (large area networks). In a multi-CRAN, the large area IoT network is divided in to several clusters of BSs. Within each cluster, the BSs are located geographically close to each other and connected to a cloud through high capacity links. This allows coordination through joint signal processing at the intracluster level. The multiple clouds (clusters) are connected to a central cloud which implements only the scheduling policy and hence, requires limited backhaul communication. Since, high speed links (optical fiber) are only required at intracloud level between geographically closed BSs, this allows for cost effectiveness, energy efficiency. In case of failure of one of the clouds, other clouds continue to operate and this results in more network reliability and robustness.

### A. Related Work

The published works on coordinated resource allocation in CRANs are mostly concentrated on a single cloud. Yu *et al.* [16] proposed scheduling of users based on proportionality fair scheme on a per-BS basis. Joint optimization of user schedule, beamforming vectors, and power spectra is performed while taking the intercell and intracell interference. Coordinated scheduling for soft frequency reuse-based networks is considered in [17]. The problem is formulated as a linear assignment with equal number of users and resource blocks (RBs), and solved using auction methodology. Douik *et al.* [18] proposed a graph theoretic approach for coordinated scheduling in the downlink of single CRAN. The users to RBs assignment is formulated as a maximum weight clique problem and solved using a heuristic algorithm. Feng *et al.* [19] considered the resource allocation problem in CRAN-based public safety network. The problem is modeled as an integer quadratic programming problem and solved using a generalized benders decomposition algorithm. Lyazidi *et al.* [20] proposed dynamic resource allocation scheme for LTE-CRAN. The problem is formulated as a mixed integer linear problem and solved using a branch and cut algorithm. Singh and Viniotis [21] proposed a resource allocation scheme based on buffering, scheduling, and rate limiting mechanism to meet the volume specific service level agreements in single cloud IoT network. Wang *et al.* [22] proposed a resource allocation technique for heterogeneous CRAN by jointly considering RBs and BBU computation resources. At first, efficient user to RBs allocation is investigated. In the next step, the BBU scheduling problem is formulated as a bin packing problem and solved with the help of a heuristic. Zhang *et al.* [23] solved the resource allocation in three tier IoT network using a game theoretic approach. Awais *et al.* [24] modeled the problem of joint allocation of users, BSs and RBs for a single CRAN and proposes a low complexity heuristic to solve it.

Multi-CRAN scenario is also considered in few works. Park *et al.* [25] addressed the coordinated scheduling problem based on a preknown association of users and clouds. The work in [26], proposed a distributed algorithm for user to cloud assignment problem in multi-CRAN scenario. Dhif-Allah *et al.* [15] modeled the distributed power minimization problem for the downlink of multi-CRANs. The optimization problem takes into account the BS power, backhaul capacity, quality of service, and CSI error constraints. Further, the problem is solved using a distributed algorithm based on alternating direction method of multipliers.

Table I provides a summary of above recent works in the domain of resource allocation in CRANs. As shown in the table, in most of the published works, a single-CRAN-based network scenario is considered. Moreover, resource allocation algorithm considers limited aspects of association (e.g., user to cloud, user to RBs, etc.). In contrast, the main contributions of proposed work are as follows.

*Contributions:*

1) To the best of our knowledge, this paper proposes the first ever framework for the resource allocation in multi-CRAN industrial IoT (MIIoT) scenario.
2) This paper considers joint allocation between users, BSs, RBs, and clouds while considering the intercloud and intracloud interference and practical network constraints.
3) An algorithm for resource allocation of MIIoT-RAN is proposed for which complexity is linear with respect to the number of BSs, number of clouds, and number of RBs, whereas it is quadratic with respect to number of IoT devices.

The rest of this paper is organized as follows. Section II describes the system model and problem formulation. Section III discusses the proposed solution for MIIoT-RAN scheduling. Simulation results are discussed in Section IV. Finally, this paper concludes in Section V.

## II. MODELING OF MIIoT-RAN

### A. System Model

Fig. 1 illustrates an example of a large scale MIIoT-RAN spread over a metropolitan city. Practically, such kind of network is composed of hundreds of heterogenous IoT devices, performing tasks in a diverse range of applications. Typical applications include smart industries, smart homes, connected vehicles, environmental monitoring, telemedicine, etc. Such network requires an extensive deployment of BSs to provide coverage to a massive number of battery constrained IoT devices. Connecting such number of geographically spaced BSs to a single cloud through high capacity links is not a cost effective solution. Moreover, it may not be possible in some cases due to infrastructural reasons or area's geographical topology.

Keeping in view of these limitations of single-CRAN, this paper considers a multi-CRAN-based IoT network scenario. The resource allocation frame work of a metropolitan area MIIoT-RAN is proposed. The considered network scenario of Fig. 1 consists of following components: 1) IoT user

TABLE I
SUMMARY OF SOME PUBLISHED WORKS ON RESOURCE ALLOCATION IN CRANS

| Work | CRAN Scenario | | Assignment Problem | Scheduling Algorithm | Application |
|---|---|---|---|---|---|
| | Single-CRAN | Multi-CRAN | | | |
| [16] | ✓ | | Users to RBs, (Users to BSs pre-known) | Proportionality Fair Heuristic | Generic CRAN |
| [17] | ✓ | | Users to RBs | Auction Based | Cellular Networks |
| [18] | ✓ | | Users to RBs | Heuristic | Generic CRAN |
| [19] | ✓ | | Users to RBs | GBD Algorithm | 5G Public Safety Network |
| [20] | ✓ | | BBU-RBs | Branch and Cut | 4G-LTE |
| [21] | ✓ | | Users to Cloud | Heuristic | IoT |
| [22] | ✓ | | Users to Cloud | Bin Packing | IoT |
| [23] | ✓ | | Users to Cloud | Game Theory | IoT+Fog Computing |
| [24] | ✓ | | Users, BSs and RBs (Joint allocation) | Heuristic | Generic CRAN |
| [25] | | ✓ | Users to RBs, (Users to Cloud pre-known) | Iterative Heuristic | Generic CRAN |
| [26] | | ✓ | Users to Clouds | Distributed Auction Based | Generic CRAN |
| This work | | ✓ | Users, Clouds, BSs and RBs (Joint allocation) | Heuristic | Industrial IoT |

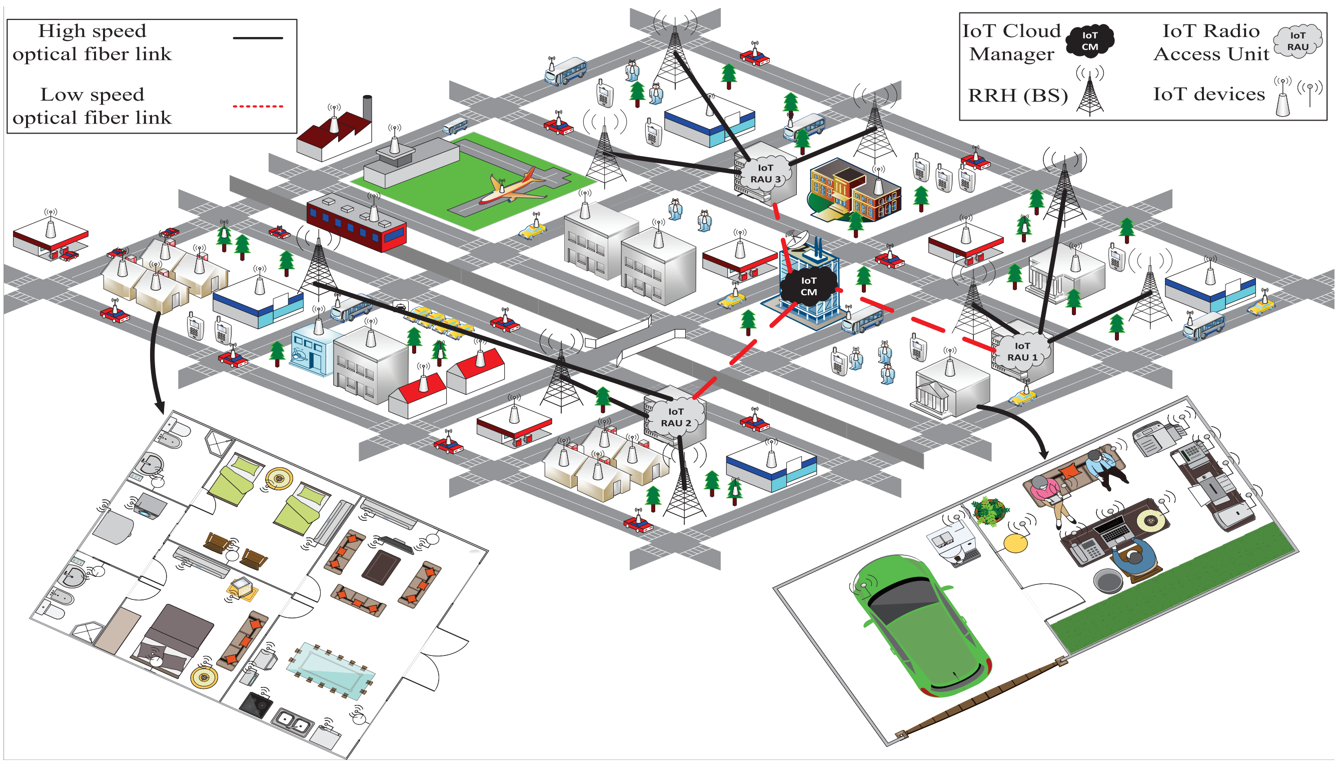


Fig. 1. Multicloud IoT radio access network.

equipments (UEs); 2) RRHs; 3) radio access units (RAUs); 4) cloud manager (CM); and 5) communication links. The transmit frame of each RRH is composed of multiple RBs. Several geographically spread RRHs are connected to a single RAU through high-speed fronthaul links. The fronthaul links are realized by different technologies, most typically with optical fiber. Each RAU is equipped with a baseband unit pool of powerful processors to process baseband signals and to optimize resource allocation. A number of RAUs are then connected to central CM which implements the UEs to RBs scheduling policy and provides synchronization of transmit frames across all connected RRHs in the network.[1]

Consider the downlink of an MIIoT-RAN which consists of $C$ clouds and serves a total of $U$ users. Each cloud is connected to $B$ BSs. Let $\mathcal{C} = \{c_1, c_2, \ldots, c_C\}$, $\mathcal{B} = \{b_1, b_2, \ldots, b_B\}$, $\mathcal{R} = \{r_1, r_2, \ldots, r_R\}$, and $\mathcal{U} = \{u_1, u_2, \ldots, u_U\}$ denote, respectively, the set of clouds, BSs per cloud, RBs per BS, and IoT devices. The total number of RBs in the network is $R_t = CBR$. The $C$ clouds are connected to the central cloud which is responsible for scheduling of all users in the network. Since the central cloud manages only scheduling level coordination, it is connected to other clouds through low capacity communication links. The MIIoT-RAN of Fig. 1 consists of three clouds, three BSs per cloud and serves a number of users. The transmission rate (bits/sec) of a wireless channel depends upon the signal-to-interference noise ratio (SINR) measured at the receiver end. The SINR of user $u$, when scheduled to RB $r$ in the transmit frame of BS $b$ of cloud $c$ is denoted by $\text{SINR}^u_{cbr}$, $\forall (c, b, r, u) \in \mathcal{C}\times\mathcal{B}\times\mathcal{R}\times\mathcal{U}$ and can be expressed as

$$\text{SINR}^u_{cbr} = \frac{P_{cbr}.\left|h^u_{cbr}\right|^2}{\Gamma\left(\sigma^2 + \sum_{(c',b')\neq(c,b)} P_{c'b'r}\left|h^u_{c'b'r}\right|^2\right)} \qquad (1)$$

[1]In the discussion that follows, we will simply call the IoT UEs as users, RRHs as BSs, RAUs as clouds and CM as central cloud.

where $P_{cbr}$ is the transmit power associated to $r$th RB of $b$th BS of $c$th cloud, $h^u_{cbr}$ is the channel gain between the $u$th IoT device and $b$th BS (associated with $r$th RB) of $c$th cloud, $\sigma^2$ is the Gaussian noise term, and $\Gamma$ is the SINR gap.

### B. MIIoT-RAN Scheduling Problem Formulation

This paper considers the MIIoT-RAN scheduling problem under the following practical constraints.

1) C1: Each user in the network can be serviced by multiple BSs in one and only one cloud.
2) C2: If a user is serviced by multiple BSs in a cloud, it must not occupy the same RBs across different BSs.
3) C3: Each RB must be allocated to at most one user.

The set $\mathcal{A} = \mathcal{C} \times \mathcal{B} \times \mathcal{R} \times \mathcal{U}$ contains all possible associations between the clouds, BSs, RBs, and IoT devices. $\mathcal{P}(\mathcal{A})$ is the power set containing all possible schedules of $\mathcal{A}$. Each individual schedule $\mathcal{S} \in \mathcal{P}(\mathcal{A})$ can be written as a set of associations, i.e., $\mathcal{S} = \{s_1, s_2, \ldots, s_{|s|}\}$, where each individual association $s_i$ is a tuple $(c, b, r, u) \in \mathcal{A}$.

We consider the following network utility maximization problem:

$$\hat{\mathbf{S}} = \arg\max_{S\in\mathcal{P}(\mathcal{A})} \sum_c \sum_b \sum_r \sum_u g_{\text{cbru}} \Omega_{\text{cbru}} \tag{2a}$$

subject to

$$\Delta_{cu} = 1 - \delta\left(\sum_{b,r} \Omega_{\text{cbru}}\right) \quad \forall (c,u) \in \mathcal{C} \times \mathcal{U} \tag{2b}$$

$$\sum_c \Delta_{cu} \le 1 \quad \forall u \in \mathcal{U} \tag{2c}$$

$$\sum_u \Omega_{\text{cbru}} = 1 \quad \forall (c,b,r) \in \mathcal{C} \times \mathcal{B} \times \mathcal{R} \tag{2d}$$

$$\nabla_{ur} = \sum_{cb} \Omega_{\text{cbru}} \le 1 \quad \forall (u,r) \in \mathcal{U} \times \mathcal{R} \tag{2e}$$

$$\Omega_{\text{cbru}}, \Delta_{cu}, \nabla_{ur} \in \{0,1\} \tag{2f}$$

where both (2b) and (2c) refer to the network constraint C1 whereas equality constraints (2d) and (2e) refer to the network constraints C2 and C3, respectively. The objective (2a) is to find among all possible schedules in $\mathcal{P}(\mathcal{A})$, an optimal schedule that maximizes the overall network utilization while satisfying constraints C1–C3. The utilization of a particular schedule $\mathcal{S} \in \mathcal{P}(\mathcal{A})$ is the sum of utilizations of individual associations in $\mathcal{S}$. $\Omega_{\text{cbru}}$ is a binary variable which is 1 if an association $s_i$ exists between a $u$th IoT user and $r$th RB of transmit frame of $b$th BS belonging to $c$th cloud, and 0 otherwise. The generic benefit achieved by the association $s_i$ is denoted by variable $g_{\text{cbru}}$ which is expressed in terms of communication rate (bits per second) of a channel formed when a user $u$ is associated with RB $r$ of $b$th BS of cloud $c$. Mathematically, it can be written as

$$g_{\text{cbru}} = \log_2(1 + \text{SINR}^u_{cbr}). \tag{3}$$

Therefore, the scheduling problem (2a) becomes the sum-rate maximization problem. In the above formulation, $\Delta_{cu}$ is a binary variable which is 1 when a user $u$ is assigned to a cloud $c$, and 0 otherwise. $\nabla_{ur}$ is another binary variable which is 1 when a user $u$ is assigned to the RB $r$ of any BS in the network, otherwise 0. $\delta(.)$ denotes the discrete dirac Delta function which is equal to 1 if its argument is equal to 0.

The existing CRAN scenarios assume either signal level coordination [25], or scheduling level coordination [16]. A signal level coordinated system is also known as a fully coordinated system. It offers maximum network utilization by connecting users to multiple BSs in different clouds. However, it requires high capacity backhaul communication links to share all data streams between different clouds. On the other hand, in simple scheduling level coordination, the users can be connected to multiple RBs of only one BS. This requires much less backhaul communications however, it suffers from poor network utilization. In typical CRAN scenarios, the clouds are connected to their BSs through high capacity links while cloud-to-cloud communication is done via low capacity (mostly wireless) links.

This paper proposes a hybrid (mixed) scheduling scheme for MIIoT network as given by the formulation (2b) to (2f). Equation (2b) enforces the first part of constraint C1, i.e., the connection of each user to atmost one cloud. Only scheduling level coordination is assumed between the clouds and the CM. Equation (2c) enforces second part of C1 and allows users to be connected to multiple BSs within a cloud. This permits coordination through joint signal coordination at intracloud level. The assumption that a user must be connected to one cloud provides a good tradeoff between network complexity and cost effectiveness. Relaxing this, would result in maximum flexibility and sum rate performance. However, it would require an extensive, high speed network deployment both at intracloud and intercloud level. This not only incurs huge deployment cost but also it is not possible in some practical cases. Moreover, C1 also makes the scheduling problem aware of intercloud interference since, a user should be connected to a cloud through which it experiences a better SINR. Similarly, intra cloud interference is handled by C2, by scheduling users to different RBs across multiple BSs.

An exhaustive search over $\mathcal{P}(\mathcal{A})$ is required to find the optimal solution. The computational complexity of such method is exponential with respect to the number of clouds, BSs, RBs, and IoT user devices, i.e., $|\mathcal{P}(\mathcal{A})| = 2^{\text{CBRU}}$. Due to the exponential computational complexity of the optimal solution, in this paper, we propose a greedy heuristic algorithm for network-wide utilization maximization in polynomial time. The detailed description is in the next section.

## III. Proposed Method for MIIoT-RAN Scheduling

In contrast to the existing works which study only limited aspects of association, this paper addresses the joint allocation problem of assigning users to clouds and scheduling them to RBs in each BS frame. This paper proposes a centralized solution to the scheduling problem formulated in the previous section. The scheduling algorithm is implemented in the CM which also manages the synchronization of transmit frames across all BSs in the network. To solve the scheduling problem, a computationally efficient method is proposed based on a greedy heuristic. The main computational steps are summarized in Algorithm 1. The cardinality of $\mathcal{C}$, $\mathcal{B}$, $\mathcal{R}$, and $\mathcal{U}$ is denoted by scalars $C$, $B$, $R$, and $U$, respectively. In addition, $N_o$ denotes the background noise power spectral density (Watts/Hz), $\Gamma$ is the SINR gap and $P_t$ is the fixed transmit power of all RBs in the system. In the first step, the algorithm performs the initialization of primary inputs and main variables. The initialization steps are given in Routine 1. The Algorithm 1 executes in four phases as discussed as follows.

*Stage 1:* At step 2, Algorithm 1 calls Routine 2, i.e., the throughput accumulation routine. At this stage, the CM computes the complex channel matrix $\mathbf{H}$ of dimensions $C \times B \times R \times U$. An entry $H_{\text{cbru}}$ represents the gain of a complex channel to be formed if a user $u$ is scheduled to the RB $r$ in the transmit frame of BS $b$ of cloud $c$. Practically, this information is provided to the CM, by each cloud in the network which has access to partial network parameters. For simulation purposes, a channel model is required which takes in to account, the frequency bandwidth, transmit power of a user, background noise, and pathloss component. This paper considers a Rayleigh fading channel which is often used as a worst case channel in many wireless situations [27]. The simulation parameters are shown in Table III. After computing the $\mathbf{H}$ matrix, the CM computes the SINR matrix $\mathbf{S}$ for all possible channels in the system, along with matrix $\mathbf{A}$ which stores their data rates. Following that, the CM performs the scheduling of users by executing stages 2–4 of Algorithm 1.

*Stage 2:* This phase guarantees a minimum network provision for all users, i.e., under the assumption $U < R_t$, which ensures the association of every user to at least one RB. The for loop runs for $U$ users, for each user the matrix $\mathbf{A}'$ is found which contains all elements of $\mathbf{A}$, excluding the elements whose user indexes are stored in $\Lambda$. Initially, $\Lambda$ is empty therefore, $\mathbf{A}' = \mathbf{A}$. In step 6, the argmax function is executed on $\mathbf{A}'$ and returns the index tuple $[c, b, r, u]$ of maximum value of $\mathbf{A}'$. The tuple $[c, b, r, u]$ shows the indices of maximum data rate channel. The value in $\mathbf{A}$ at the indexes $[c, b, r, u]$ is preserved to mark an association between user $u$ and RB $r$ of BS $b$ of cloud $c$. Steps 7–9 ensure that constraints C1–C3, respectively, are met for this association. In step 10, the user index returned by the argmax function is concatenated with $\Lambda$, i.e., added to the list of users which are to be excluded from argmax function in the next iteration.

In Fig. 2, execution of proposed algorithm is illustrated with the help of an example for an MIIoT-RAN configuration with $C = 2, B = 2, R = 3,$ *and* $U = 3$. Fig. 2(a) shows the outcome of stage 1, i.e., $\mathbf{A}$ matrix. For ease of demonstration, the structure of $\mathbf{A}$ matrix is illustrated such that the pages correspond to the elements of set $\mathcal{C}$ whereas, each page contains a submatrix whose rows correspond to the elements of set $\mathcal{U}$ whereas, the columns correspond to the elements of set $\mathcal{B} \times \mathcal{R}$. Fig. 2(b)–(d) shows the steps performed by all iterations of stage 2.

*Stage 3:* This phase assigns the remaining $R_t - U$ RBs to the users. The $\mathbf{A}$ matrix is updated column-wise such that for each column (RB) $\mathbf{u} \in \mathcal{C} \times \mathcal{B} \times \mathcal{R}$, the maximum at row (user) index $u$ is preserved to mark an association between RB $\mathbf{u}$ and user $u$. Steps 15 and 16 ensure that constraints C2 and C3 are satisfied for this association. This process is shown in Fig. 2(e).

**Algorithm 1** Proposed for MIIoT-RAN Scheduling

1: **Routine 1: Inputs and Initialization**
2: **Stage 1: Routine 2: Throughput accumulation**
3: **Stage 2:**
4: **for** $i = 1$ to $U$ **do**
5: $\quad \mathbf{A}'_{cbru} \leftarrow \mathbf{A}_{cbru},\ \forall c,\ b,\ r,\ u \backslash \Lambda$
6: $\quad [c, b, r, u] \leftarrow \text{argmax}(\mathbf{A}')$
7: $\quad \mathbf{A}_{c'b'r'u} \leftarrow 0,\ \forall\, c' \in \mathcal{C} \backslash c, b' \in \mathcal{B},\ r' \in \mathcal{R}$
8: $\quad \mathbf{A}_{cb'ru} \leftarrow 0,\ \forall b' \in \mathcal{B} \backslash b$
9: $\quad \mathbf{A}_{c'bru} \leftarrow 0,\ \forall\, u' \in \mathcal{U} \backslash u$
10: $\quad \Lambda \leftarrow \{\Lambda, u\}$
11: **end for**
12: **Stage 3:**
13: **for** $\forall c,\ b,\ r$ **do**
14: $\quad \mathbf{u} \leftarrow \mathbf{A}_{cbru'},\ \forall\, u' \in \mathcal{U}$
15: $\quad [u] \leftarrow \text{argmax}(\mathbf{u})$
16: $\quad \mathbf{A}_{cb'ru} \leftarrow 0,\ \forall\, b' \in \mathcal{B} \backslash b$
17: **end for**
18: **Stage 4:** $\forall c \in \mathcal{C},\ b \in \mathcal{B},\ r \in \mathcal{R},\ u \in \mathcal{U}$
19: $\hat{\mathbf{A}}_{cbru} \leftarrow 1,$ if $\mathbf{A}_{cbru} \neq 0;\ a \leftarrow \sum_c \sum_b \sum_r \sum_u \mathbf{A}$
20: **Outputs:** $a,\ \hat{\mathbf{A}}$

**Algorithm 2** Optimal Algorithm for MIIoT-RAN Scheduling

1: **Routine 1: Inputs and Initialization**
2: **Stage 1: Routine 2: Throughput accumulation**
3: **Stage 2:**
4: **for** $i \leftarrow 0, 2^{C \cdot B \cdot R \cdot U} - 1$ **do**
5: $\quad a' \leftarrow 0$
6: $\quad \Omega \leftarrow \text{getbin}(i)$
7: $\quad a' \leftarrow \begin{cases} \arg\max\limits_{S \in \mathcal{P}(\mathcal{A})} \sum\limits_{c,b,r,u} \mathbf{A}_{cbru}\Omega_{cbru}, & \forall c,\ b,\ r,\ u \\ \text{subject to:} \quad \text{(2b) to (2e)} \end{cases}$
8: $\quad$ **if** $a' > a$ **then**
9: $\quad\quad a \leftarrow a'$
10: $\quad\quad \hat{\mathbf{A}}_{cbru} \leftarrow \Omega_{cbru},\ \ \forall c,\ b,\ r,\ u$
11: $\quad$ **end if**
12: **end for**
13: **Outputs:** $a,\ \hat{\mathbf{A}}$

**Routine 1** Inputs and Initialization

1: **Inputs:**
2: $C,\ B,\ R,\ U,\ N_o,\ \Gamma,\ P_t$
3: $\mathcal{C} = \{1, 2, 3, \cdots, C\},\ \mathcal{B} = \{1, 2, 3, \cdots, B\},\ \mathcal{R} = \{1, 2, 3, \cdots, R\},\ \mathcal{U} = \{1, 2, 3, \cdots, U\}$
4: **Initialize:** $\forall\ c \in \mathcal{C},\ b \in \mathcal{B},\ r \in \mathcal{R},\ u \in \mathcal{U}$
5: $\mathbf{H}_{cbru} \leftarrow 0,\ \mathbf{S}_{cbru} \leftarrow 0,\ \mathbf{A}_{cbru} \leftarrow 0,\ \hat{\mathbf{A}}_{cbru} \leftarrow 0,\ \Lambda \leftarrow \phi$

**Routine 2** Throughput Accumulation

1: $\forall\ c \in \mathcal{C},\ b \in \mathcal{B},\ r \in \mathcal{R},\ u \in \mathcal{U}$
2: $\mathbf{H}_{cbru} \leftarrow \text{getchannel}(\cdot)$
3: $\mathbf{S}_{cbru} \leftarrow \dfrac{P_t.|\mathbf{H}_{cbru}|^2}{\Gamma.\left(\sqrt{2.N_0}.\text{rand}(\cdot) + \sum\limits_{\substack{c' \in \mathcal{C} \backslash c \\ b' \in \mathcal{B} \backslash b}} P_t.|\mathbf{H}_{c'b'ru}|^2\right)}$
4: $\mathbf{A}_{cbru} \leftarrow \log_2(1 + \mathbf{S}_{cbru})$

*Stage 4:* In this phase, the output binary schedule matrix $\hat{\mathbf{A}}$ is computed based on nonzero entries of $\mathbf{A}$. Finally, the entries of $\mathbf{A}$ are added to get the overall network sum rate $a$. Finally, the CM communicates the scheduling decisions to each cloud which includes the users associated to them along with their

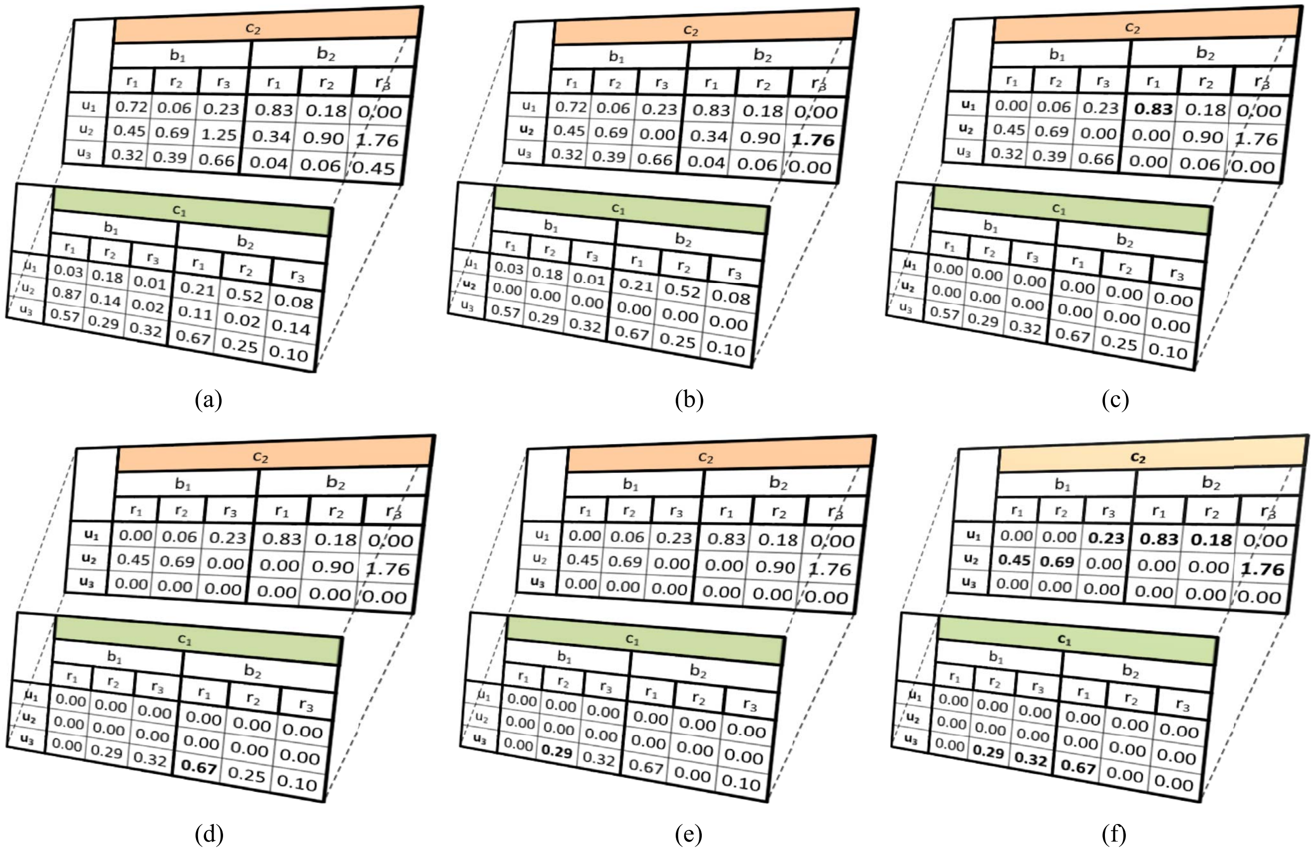


Fig. 2. Example for Algorithm 1 for an MIIoT-RAN scheduling consisting of $B = 3, R = 2$, and $U = 3$.ac. (a) Stage 1: matrix $\mathbf{A}$; the pages correspond to the elements of set $\mathcal{C}$ whereas, in each page the rows correspond to the elements of set $\mathcal{U}$ and columns correspond to the elements of set $\mathcal{B} \times \mathcal{R}$. (b) Stage 2: steps 4–10. $i = 1$, $\Lambda$ is initially empty therefore $\mathbf{A}' = \mathbf{A}$. The argmax($\mathbf{A}'$) returns indexes tuple $[c, b, r, u] = [2, 2, 3, 2]$ for maximum value 1.76. RB $c_2b_2r_3$ is assigned to $u_2$. To satisfy C1–C3, respectively, all RBs of cloud $c_1$ are marked zero for $u_2$, RB $c_2b_1r_3$ of $c_2$ is marked zero for $u_2$ and RB $c_2b_2r_3$is marked zero for users $u_1$and $u_3$. $\Lambda = \{2\}$. (c) Stage 2: steps 4–10. $i = 2$, $\Lambda = \{2\}$.$\mathbf{A}'$ contains all elements of $\mathbf{A}$ except those with user index 2 (i.e., second row). The argmax($\mathbf{A}'$) returns indexes tuple $[c, b, r, u] = [2, 2, 1, 1]$ for maximum value 0.83. RB $c_2b_2r_1$ is assigned to $u_1$. To satisfy C1–C3, respectively, all RBs of cloud $c_1$ are marked zero for $u_1$, RB $c_2b_1r_1$ is marked zero for $u_2$ and RB $c_2b_2r_1$ is marked zero for users $u_2$ and $u_3$. $\Lambda = \{2, 1\}$. (d) Stage 2: steps 4–10. $i = 3$, $\Lambda = \{1, 2\}$.$\mathbf{A}'$ contains all elements of $\mathbf{A}$ except those with user index 1 and 2 (i.e., first and second row). The argmax($\mathbf{A}'$) returns indexes tuple $[c, b, r, u] = [1, 2, 1, 3]$ for maximum value 0.67. RB $c_1b_2r_1$ is assigned to $u_3$. To satisfy C1–C3, respectively, all RBs of cloud $c_2$ are marked zero for $u_3$, RB $c_1b_1r_1$ is marked zero for $u_3$ and RB $c_1b_2r_1$ is marked zero for users $u_1$and $u_2$. $\Lambda = \{2, 1, 3\}$. (e) Stage 3: steps 13–17. The RB $c_1b_1r_2$ has maximum rate for $u_3$and therefore, assigned. To satisfy C2 and C3, respectively, RB $c_1b_2r_2$ is marked zero for $u_3$ and RB $c_1b_1r_2$is marked zero for users $u_1$and $u_2$. This process continues for all RBs $u \in \mathcal{C} \times \mathcal{B} \times \mathcal{R}$. (f) Updated $\mathbf{A}$ matrix at the end of stage 3.

allocated BSs and RBs. At intracloud level, the transmission of users connected to multiple BSs is coordinated by their respected cloud, by performing joint signal processing.

### *A. Optimal Algorithm*

Algorithm 2 lists the main steps of an optimal resource allocation algorithm based on an exhaustive search. The first two steps of the algorithm are same as that of Algorithm 1.

*Stage 2:* This iterative stage runs through the maximum search space, i.e., $2^{C \cdot B \cdot R \cdot U}$ iterations. A binary candidate schedule matrix $\Omega$ is of dimensions $C \times B \times R \times U$ is generated in each iteration. The practical constraints C1, C2, and C3 are tested for this candidate and a local rate matrix $\mathbf{A}'$ is obtained by performing a dot product of matrices $\Omega$ and $\mathbf{A}$ for all feasible candidates. The local sum rate $a'$ is obtained by computing the commutative sum of individual entries of $\mathbf{A}'$. The overall sum rate $a$ is updated with $a'$ and the local binary search $\Omega$ is updated with $\hat{\mathbf{A}}$ if the local sum rate $a'$ is better than the overall sum rate $a$.

### *B. Complexity Analysis*

The main advantage of the proposed method is its low computational complexity, where the complexity is calculated in terms of flops. Table II presents the step by step complexity analysis of the proposed algorithm. The initialization phase of Algorithm 1 has a total complexity equal to 4CBRU + 1 flops. The stage 1 runs for CBRU iterations. The complexity per iteration of step 7 is 2. The complexity per iteration of numerator term of step 8 is 5 flops whereas, the complexity per iteration of denominator term is 5CB + 6. The total complexity per iteration of step 8 is (5CB + 12). The overall complexity of all iterations of stage 1 is CBRU(5CB + 16). The stage 2 runs for $U$ iterations whose overall complexity is $U(2\text{CBRU} + (C - 1)BR + B + U - 1)$. Similarly, Table II also shows the complexity of individual steps of stages 3 and 4 which have complexities $\text{CBR}(2U + B)$ and 3CBRU, respectively. The proposed algorithm requires $\text{CBRU}(5\text{CB} + 2U + 26) + BR(\text{CB} - U) + U(B + U - 1) - 1$ flops.

TABLE II
COMPLEXITY ANALYSIS OF PROPOSED HEURISTIC ALGORITHM

| Phase | Computation Step | Complexity (Flops) |
|---|---|---|
| Initialization Phase | Loop : $\forall c,\ b,\ r,\ u$<br>$\mathbf{H_{cbru}} \leftarrow 0, \mathbf{S}_{cbru} \leftarrow 0, \mathbf{A}_{cbru} \leftarrow 0, \mathbf{A}_{\hat{cbru}} \leftarrow 0\ \Lambda \leftarrow \phi$ | $4CBRU + 1$ |
| Stage 1 | Loop : $\forall c,\ b,\ r,\ u$<br>$\mathbf{H_{cbru}} \leftarrow$ getchannel()<br>$\mathbf{S}_{cbru} \leftarrow \frac{P_t \cdot \lvert \mathbf{H}_{cbru} \rvert^2}{\Gamma \cdot \left( \sqrt{2 \cdot N_0} \cdot \mathrm{rand}(\cdot) + \sum_{\substack{c' \in \mathcal{C} \backslash c \\ b' \in \mathcal{B} \backslash b}} P_t \cdot \lvert \mathbf{H}_{c'b'ru} \rvert^2 \right)}$<br>$\mathbf{A}_{cbru} \leftarrow \log_2(1 + \mathbf{S}_{cbru})$ | $CBRU(5CB + 16)$ |
| Stage 2 | Loop : For $i = 1$ to $U$<br>$\mathbf{A}'_{cbru} \leftarrow \mathbf{A}_{cbru},\ \forall c,\ b,\ r,\ u \backslash \Lambda$<br>$[c, b, r, u] \leftarrow \mathrm{argmax}(\mathbf{A}')$<br>$\mathbf{A}_{c'b'r'u} \leftarrow 0,\ \forall\, c' \in \mathcal{C} \backslash c, b' \in \mathcal{B}, r' \in \mathcal{R}$<br>$\mathbf{A}_{cb'ru} \leftarrow 0,\ \forall b' \in \mathcal{B} \backslash b$<br>$\mathbf{A}_{c'bru} \leftarrow 0,\ \forall\, u' \in \mathcal{U} \backslash u$<br>$\Lambda \leftarrow \{\Lambda, u\}$ | $U(2CBRU + (C-1)BR + B + U - 1)$ |
| Stage 3 | Loop: $\forall c,\ b,\ r$<br>$\mathbf{u} \leftarrow \mathbf{A}_{cbru'},\ \forall\, u' \in \mathcal{U}$<br>$[u] \leftarrow \mathrm{argmax}(\mathbf{u})$<br>$\mathbf{A}_{cb'ru} \leftarrow 0,\ \forall\, b' \in \mathcal{B} \backslash b$ | $CBR(2U + B)$ |
| Stage 4 | Loop : $\forall c,\ b,\ r,\ u$<br>$\hat{\mathbf{A}}_{cbru} \leftarrow 1,$ if $\mathbf{A}_{cbru} \neq 0$<br>$a \leftarrow \sum_{cbru} \mathbf{A}$ | $3CBRU$ |
| Overall complexity of the proposed algorithm $= CBRU(5CB + 2U + 26) + BR(CB - U) + U(B + U - 1) - 1 \approx O(CBU^2R)$ | | |

From the total number of flops, we can deduce the complexity of the proposed algorithm as $O(C^2B^2\mathrm{RU} + \mathrm{CBRU}^2 + B^2 + \mathrm{CB}^2R - \mathrm{BRU} + \mathrm{BU} + U^2 - U) \approx O(\mathrm{CBRU}(\mathrm{CB} + U)) \approx O(\mathrm{CBU}^2R)$ as $U \gg BC$. Therefore, the complexity of the proposed algorithm is linear with respect to $C$, $R$, and $B$, and quadratic with respect to $U$, i.e., IoT devices. With the same system model and constraints C1–C3, the computational complexity of the optimal algorithm (Algorithm 2) is $O(2^{\mathrm{CBRU}})$.

## IV. SIMULATION RESULTS

In this section, the simulation results of the proposed resource allocation algorithm are presented. The multicloud assisted IoT network scenario is similar to the one shown in Fig. 1 and optimization is performed over the sum rate (bits/sec/Hz) maximization problem. The important parameters of the simulation setup are reported in Table III. The number of RAUs (IoT clouds), IoT devices, RRHs (BSs) per RAU, and RBs per RRH are kept variable in order to analyze the performance of proposed method for various scenarios. The users are uniformly placed in the network. The Rayleigh channel path loss model is adopted which simulates the worst case scenario. For each network configuration, the simulation results reported are the average results of Monte Carlo iterations.

At first, the sum rate results of proposed solution (Algorithm 1) are compared with the brute force algorithm based on an exhaustive search (Algorithm 2). Due to exponential increase in search space with network size, only few small sized network scenarios are simulated with optimal search and results are reported in Fig. 3. The simulation results of Fig. 3 show that the proposed algorithm performs close to the optimal algorithm. This verifies the accuracy of the proposed solution and its validity for practical sized IoT networks.

TABLE III
MAIN SIMULATION PARAMETERS OF ALGORITHM 1

| | |
|---|---|
| No. of IoT RAUs (C) | variable |
| No. of RRHs (B) per cloud | variable |
| No. of IoT devices (U) | variable |
| No. of RBs per RRH(R) | variable |
| Maximum transmit power per RB ($P_t$) | $-42.60$dBm/Hz |
| Noise | $-168.60$dBm/Hz |
| Signal to noise ratio gap ($\Gamma$) | 0dB |
| Path loss model | Rayleigh |
| Bandwidth | 1MHz |

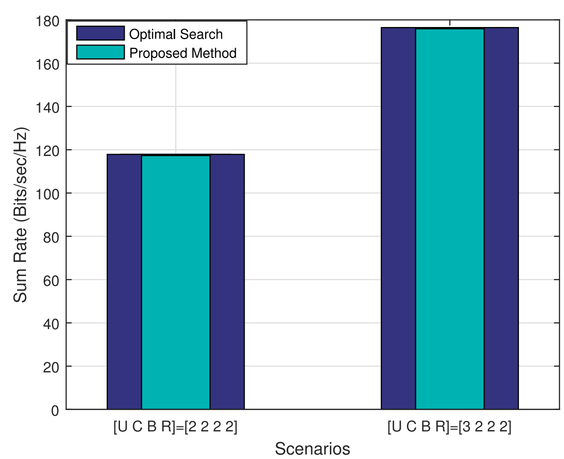


Fig. 3. Sum rate (bits/sec/Hz) comparison of proposed method (Algorithm 1) and optimal search method (Algorithm 2) for various scenarios.

Fig. 4(a) plots the sum rate of the proposed method for a more practical IoT network. The sum rate is plotted as a function of number of IoT devices ranging from $U = 25$ to 200, distributed uniformly across the network. Different network configurations are simulated in which the number of

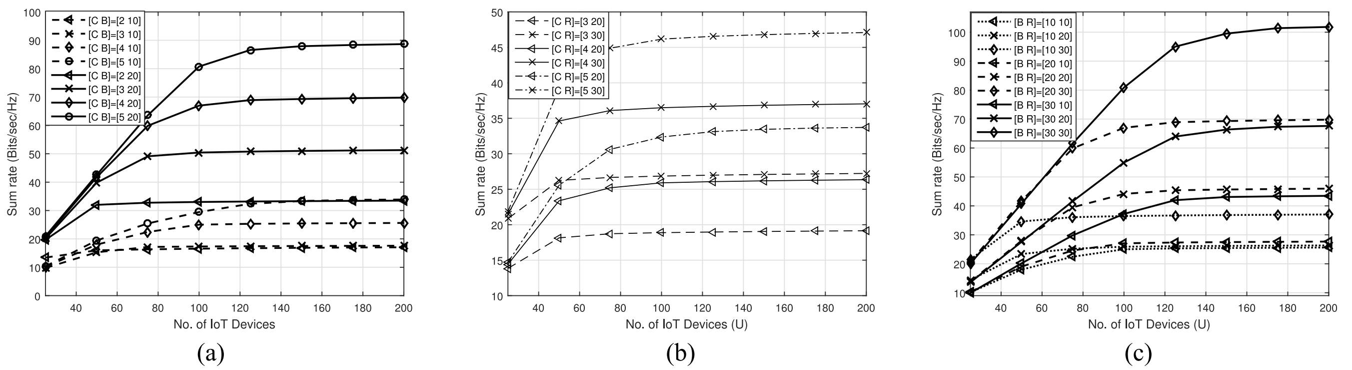


Fig. 4. Sum rate (bits/sec/Hz) simulation results of proposed algorithm for various IoT network scenarios. (a) RBs per BS are 10. (b) BSs per cloud are 10. (c) Number of clouds is 4.

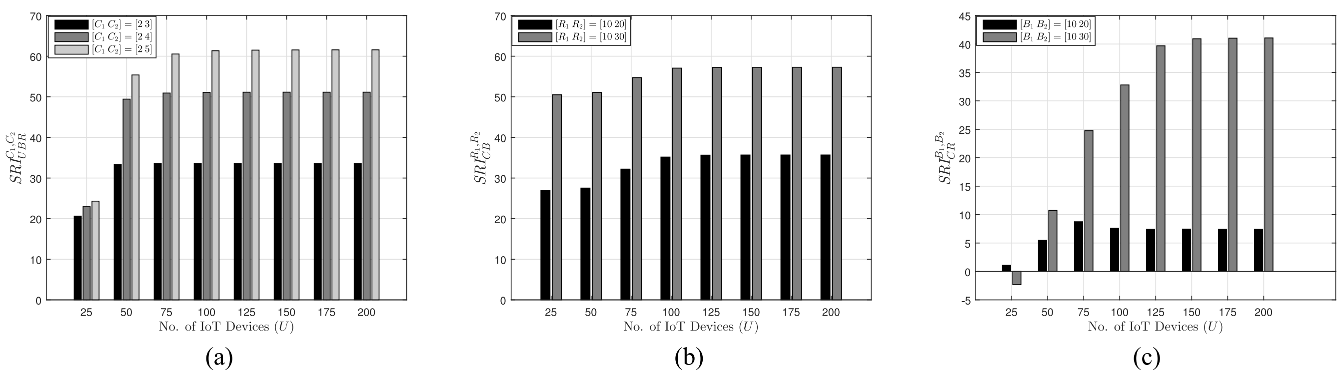


Fig. 5. SRI as function of number of IoT devices ($U$) for various scenarios. (a) $B = 10$ and $R = 30$. (b) $B = 30$ and $C = 3$. (c) $R = 30$ and $C = 3$.

IoT clouds ranges from $C = 2$ to 5 and the number of BSs per cloud is $B = 10$ and 20. The number of RBs per BS is fixed, i.e., $R = 10$. The plots reveal a number of trends. First, given a fixed value of $B$, $R$, and $U << R_t$, increasing the number of clouds alone does not result in significant improvement in sum rate. This is shown by the points in graph for $U = 25$ and 50 for two cases corresponding to $B = 10$ and 20. For each case, the sum rates achieved by the numbers of clouds from $C = 2$ to 5 are fairly close to each other. This is due to the network constraint C1, i.e., a user must be serviced by only one cloud at a time. For larger values of $U$, the sum rate increases with increase in $C$ and $B$. However, keeping $U$ and $R$ fixed, the sum rate achieved by increasing the value of $B$ alone is almost twice the sum rate achieved by increasing the value of $C$ alone. This is because a user can be serviced possibly by multiple BSs within a cloud (constraint C1). Since a user must be allocated different RBs across multiple BSs in a cloud (constraint C2), the intracloud interference experienced by a user is avoided, resulting in better overall network utilization. For given values of $C, B$, and $R$, the sum rate increases sharply as a function of $U$ for small values of $U$. For large values of $U \approx R_t$, the sum rate increases only slightly with $U$. This is due to the fact that when the number of IoT devices is large, the probability that devices are scheduled to different clouds increases, which then increases the chance of intracloud interference especially in strong shadowing environments. Therefore, in practical IoT networks with large number of devices, the role of scheduling algorithm at the central cloud becomes more pronounced as a technique to achieve reasonable sum rate while minimizing the interference.

In Fig. 4(b), the simulation results are demonstrated for fixed number of BSs per cloud, i.e., $B = 10$. The sum rate is plotted as a function of $U$ with $C$ ranging from 3 to 5 and $R$ ranging from 10 to 30. The plots reveal that for fixed $U$ and $B$, the sum rate increases by increasing $C$ and $R$. However, increase in sum rate by increasing $C$ alone is more pronounced as compared to the sum rate increase obtained by increasing $R$ alone. This is due to the fact that increasing the number of clouds ($C$) increases the total number of RBs, i.e., $R_t$ available in the network. Fig. 4(b) also illustrates that jointly increasing $C$ and $R$ results in significant increase in sum rate. In Fig. 4(c), the sum rate of the proposed solution is plotted as a function of $U$ for fixed number of clouds $C = 4$ with $B$ and $R$ both ranging from 10 to 30. A similar trend is observed, that given fixed $C$ and $U$, the sum rate increases more significantly by increasing $B$ as compared to increasing $R$ alone.

In order to quantify the effect of parameters $U, C, B$, and $R$ on network sum rate, a performance metric named as sum rate improvement (SRI) is introduced in this paper. The notation $\mathrm{SRI}^{z_1,z_2}_{x,y}$ is adopted which denotes the percentage improvement in sum rate of a network with fixed parameters $x$ and $y$ and variable parameter $z$ whose value changes from $z = z_1$ to $z_2$. In Fig. 5(a), the $\mathrm{SRI}^{C_1,C_2}_{B,R}$ is plotted as a function of $U$ for a network with $B = 10$ and $R = 30$ and increasing $C$ from $C_1 = 2$ to $C_2$ up to 5. It is observed that for fixed small number of IoT devices ($U << R_T$), the sum rate improves slightly by increasing $C$. However, for larger value of $U$, a significant SRI is achieved by increasing the number of clouds $C$ from 2 to 5. Moreover, the SRI is also positive and almost same for large number of IoT devices ($U$), which demonstrates the accuracy of the proposed solution. In Fig. 5(b), the $\mathrm{SRI}_{B,C}^{R_1,R_2}$ is plotted as a function of $U$ for $B = 30$, $C = 3$, and variable $R$. A similar trend is observed, i.e., increasing the number of RBs per BS from $R_1 = 10$ to $R_2 = 20$ and 30 results in significant SRI for all values of $U < R_T$. Finally, Fig. 5(c) plots the $\mathrm{SRI}_{R,C}^{B_1,B_2}$ as a function of $U$ when $R$ and $C$ are fixed to 30 and 3, respectively, and $B$ changes from $B_1 = 10$ to $B_2 = 20$ and 30. Again, the plots of Fig. 5(c) reveal a significant, positive SRI with respect to increasing the number of BSs per cloud ($B$).

## V. Conclusion

Massive deployment of IoT devices in practical IoT networks is challenging because of the limited spectrum availability and requirements of high data rate, traffic volume, and energy efficiency. This calls for integration of IoT systems with emerging cellular communications especially 5G. Cloud-based radio access is a key technology to provide energy efficient support for a large number of devices. In this paper, we investigated the scheduling of IoT devices in multicloud IoT network. A downlink RAN scenario is considered in which a central cloud is connected to multiple clouds, each of them is then connected to a number of BSs. The transmit frame of each BS is divided in to a number of RBs. The IoT devices to RBs assignment problem is solved combinatorially under practical network constraints. However, the size of search space is exponential in the network size. To solve this problem in linear time, we proposed an efficient heuristic greedy algorithm. The simulation results are reported for a number of practical network scenarios. The proposed solution not only performs close to the optimal one but is also computationally efficient. The simulation results verify the applicability of the proposed solution for large scale IoT networks.

## References


[1] X. Lu, I. H. Kim, A. Xhafa, J. Zhou, and K. Tsai, "Reaching 10-years of battery life for industrial IoT wireless sensor networks," in *Proc. Symp. VLSI Circuits*, Jun. 2017, pp. C66–C67.

[2] T. Farnham, "Proactive wireless sensor network for industrial IoT," in *Proc. IEEE Int. Conf. Commun. (ICC)*, May 2017, pp. 1–6.

[3] C.-T. Cheng, N. Ganganath, and K.-Y. Fok, "Concurrent data collection trees for IoT applications," *IEEE Trans. Ind. Informat.*, vol. 13, no. 2, pp. 793–799, Apr. 2017.

[4] S. Rao and R. Shorey, "Efficient device-to-device association and data aggregation in industrial IoT systems," in *Proc. 9th Int. Conf. Commun. Syst. Netw. (COMSNETS)*, Jan. 2017, pp. 314–321.

[5] F. Civerchia *et al.*, "Industrial Internet of Things monitoring solution for advanced predictive maintenance applications," *J. Ind. Inf. Integr.*, vol. 7, pp. 4–12, Sep. 2017.

[6] O. Givehchi, K. Landsdorf, P. Simoens, and A. W. Colombo, "Interoperability for industrial cyber-physical systems: An approach for legacy systems," *IEEE Trans. Ind. Informat.*, vol. 13, no. 6, pp. 3370–3378, Dec. 2017.

[7] F. G. Brundu *et al.*, "IoT software infrastructure for energy management and simulation in smart cities," *IEEE Trans. Ind. Informat.*, vol. 13, no. 2, pp. 832–840, Apr. 2017.

[8] A. Esfahani *et al.*, "A lightweight authentication mechanism for M2M communications in industrial IoT environment," *IEEE Internet Things J.*, to be published.

[9] O. Galinina, S. Andreev, M. Komarov, and S. Maltseva, "Leveraging heterogeneous device connectivity in a converged 5G-IoT ecosystem," *Comput. Netw.*, vol. 128, pp. 123–132, Dec. 2017.

[10] K. Zeman *et al.*, "Wireless M-BUS in industrial IoT: Technology overview and prototype implementation," in *Proc. 23rd Eur. Wireless Conf. Eur. Wireless*, May 2017, pp. 1–6.

[11] T.-H. Kim, C. Ramos, and S. Mohammed, "Smart city and IoT," *Future Gener. Comput. Syst.*, vol. 76, pp. 159–162, Nov. 2017.

[12] Y. Yang, X. Liu, and R. H. Deng, "Lightweight break-glass access control system for healthcare Internet-of-Things," *IEEE Trans. Ind. Informat.*, vol. 14, no. 8, pp. 3610–3617, Aug. 2018.

[13] H. Kanzaki, K. Schubert, and N. Bambos, "Video streaming schemes for industrial IoT," in *Proc. 26th Int. Conf. Comput. Commun. Netw. (ICCCN)*, Jul. 2017, pp. 1–7.

[14] M. I. Ashraf, C.-F. Liu, M. Bennis, and W. Saad, "Towards low-latency and ultra-reliable vehicle-to-vehicle communication," in *Proc. Eur. Conf. Netw. Commun. (EuCNC)*, Jun. 2017, pp. 1–5.

[15] O. Dhif-Allah, H. Dahrouj, T. Y. Al-Naffouri, and M. S. Alouini, "Distributed robust power minimization for the downlink of multi-cloud radio access networks," *IEEE Trans. Cogn. Commun. Netw.*, vol. 2, no. 2, pp. 327–335, Jun. 2018.

[16] W. Yu, T. Kwon, and C. Shin, "Multicell coordination via joint scheduling, beamforming, and power spectrum adaptation," *IEEE Trans. Wireless Commun.*, vol. 12, no. 7, pp. 1–14, Jul. 2013.

[17] H. Dahrouj, W. Yu, T. Tang, J. Chow, and R. Selea, "Coordinated scheduling for wireless backhaul networks with soft frequency reuse," in *Proc. 21st Eur. Signal Process. Conf. (EUSIPCO)*, Sep. 2013, pp. 1–5.

[18] A. Douik, H. Dahrouj, T. Y. Al-Naffouri, and M.-S. Alouini, "Coordinated scheduling for the downlink of cloud radio-access networks," in *Proc. IEEE Int. Conf. Commun. (ICC)*, Jun. 2015, pp. 2906–2911.

[19] L. Feng, W. Li, P. Yu, and X. Qiu, "An enhanced OFDM resource allocation algorithm in C-RAN based 5G public safety network," *Hindawi J. Mobile Inf. Syst.*, vol. 2016, no. 7, pp. 1–14.

[20] M. Y. Lyazidi, N. Aitsaadi, and R. Langar, "Dynamic resource allocation for cloud-ran in LTE with real-time BBU/RRH assignment," in *Proc. IEEE Int. Conf. Commun. (ICC)*, May 2016, pp. 1–6.

[21] A. Singh and Y. Viniotis, "Resource allocation for IoT applications in cloud environments," in *Proc. Int. Conf. Comput. Netw. Commun. (ICNC)*, Jan. 2017, pp. 719–723.

[22] K. Wang, W. Zhou, and S. Mao, "On joint BBU/RRH resource allocation in heterogeneous cloud-RANs," *IEEE Internet Things J.*, vol. 4, no. 3, pp. 749–759, Jun. 2017.

[23] H. Zhang *et al.*, "Computing resource allocation in three-tier IoT fog networks: A joint optimization approach combining Stackelberg game and matching," *IEEE Internet Things J.*, vol. 4, no. 5, pp. 1204–1215, Oct. 2017.

[24] M. Awais *et al.*, "Efficient joint user association and resource allocation for cloud radio access networks," *IEEE Access*, vol. 5, pp. 1439–1448, 2017.

[25] S.-H. Park, O. Simeone, O. Sahin, and S. Shamai, "Inter-cluster design of precoding and fronthaul compression for cloud radio access networks," *IEEE Wireless Commun. Lett.*, vol. 3, no. 4, pp. 369–372, Aug. 2014.

[26] H. Dahrouj, T. Y. Al-Naffouri, and M.-S. Alouini, "Distributed cloud association in downlink multicloud radio access networks," in *Proc. 49th Annu. Conf. Inf. Sci. Syst. (CISS)*, Mar. 2015, pp. 1–3.

[27] J. Aráuz, P. Krishnamurthy, and M. A. Labrador, "Discrete Rayleigh fading channel modeling," *Wireless Commun. Mobile Comput.*, vol. 4, no. 4, pp. 413–425, 2004.



**Muhammad Awais** received the M.S. and Ph.D. degrees from the VLSI Lab, Politecnico di Torino, Turin, Italy, in 2010 and 2014, respectively.

Since 2014, he has been affiliated as an Assistant Professor with the Electrical Engineering Department, COMSATS University Islamabad (Wah Campus), Wah Cantonment, Pakistan. His current research interests include design and optimization of algorithms for 5G communications, design for advanced channel decoders, digital design using beyond CMOS technologies, and reversible computing.

**Ashfaq Ahmed** received the M.Sc. and Ph.D. degree from the Department of Electronics and Telecommunications, Politecnico di Torino, Turin, Italy, in 2010 and 2014, respectively.

He is currently an Assistant Professor with the Department of Electrical and Computer Engineering, COMSATS University Islamabad (Wah Campus), Wah Cantonment, Pakistan. His current research interests include applied optimization, targeting telecommunication and smart system applications, ASICs and FPGA design and implementation of digital signal processing architectures, especially the areas closely related to digital communications and video and image coding.

**Syed Azhar Ali** received the Ph.D. degree in electronics and telecommunications engineering from the Politecnico di Torino, Turin, Italy.

He is an Assistant Professor with the Department of Electronic Engineering, University of Engineering and Technology at Taxila, Taxila, Pakistan. His current research interests include implementation of architectures for digital signal processing and communications.

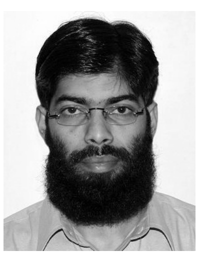

**Muhammad Naeem** received the B.S. and M.S. degrees in electrical engineering from the University of Engineering and Technology at Taxila, Taxila, Pakistan, in 2000 and 2005, respectively, and the Ph.D. degree from Simon Fraser University, Burnaby, BC, Canada, in 2011.

From 2012 to 2013, he was a Post-Doctoral Research Associate with the WINCORE Lab, Ryerson University, Toronto, ON, Canada. He is currently an Associate Professor with the Department of Electrical and Computer Engineering, COMSATS University Islamabad (Wah Campus), Wah Cantonment, Pakistan. From 2000 to 2005, he was a Senior Design Engineer with Comcept (pvt) Ltd., Islamabad, Pakistan. At the design Department of Comcept (pvt) Ltd., he participated in the design and development of smart card-based GSM and CDMA pay phones. He is also a Microsoft Certified Solution Developer. His current research interests include optimization of wireless communication systems, nonconvex optimization, resource allocation in cognitive radio networks, and approximation algorithms for mixed integer programming in communication systems.

Dr. Naeem was a recipient of the NSERC CGS Scholarship.

**Waleed Ejaz** (S'12–M'14–SM'16) received the B.Sc. degree in computer engineering from the University of Engineering and Technology at Taxila, Taxila, Pakistan, the M.Sc. degree in computer engineering from the National University of Sciences and Technology, Islamabad, Pakistan, and the Ph.D. degree in information and communication engineering from Sejong University, Seoul, South Korea, in 2014. He also completed certificate courses on Teaching and Learning in Higher Education at the Chang School, Ryerson University, Toronto, ON, Canada.

He is an Assistant Professor with Thompson Rivers University, Kamloops, BC, Canada. Since 2014, he held academic and research positions with Ryerson University, Carleton University, Ottawa, ON, Canada, and Queen's University, Kingston, ON, Canada. His current research interests include Internet of Things, energy harvesting, 5G cellular networks, and mobile cloud computing.

Dr. Ejaz's professional activities include being an Associate Editor of the *IEEE Communications Magazine*, IEEE CANADIAN JOURNAL OF ELECTRICAL AND COMPUTER ENGINEERING, and IEEE ACCESS. He has also handled several special issues of prestigious journals, as well as being on Organizing Committees of several major IEEE conferences and workshops. He is a registered Professional Engineer in the Province of British Coloumbia, Canada.

**Alagan Anpalagan** received the B.A.Sc., M.A.Sc., and Ph.D. degrees in electrical engineering from the University of Toronto, Toronto, ON, Canada. He also completed a course on Project Management for Scientist and Engineers at the University of Oxford CPD Center, Oxford, U.K.

He joined the Department of Electrical and Computer Engineering, Ryerson University, Toronto, in 2001, and became to a Full Professor in 2010, where he directs a research group involved with radio resource management and radio access and networking areas within the WINCORE Lab. He has co-authored/edited *Small Cell Networks* (Cambridge Univ. Press, 2014), *Handbook of Green Information and Communication Systems* (Academic, 2012), and *Routing in Opportunistic Networks* (Springer-Verlag, 2013). He has authored or co-authored over 200 technical papers. His current research interests include cognitive radio resource allocation and management, wireless cross layer design and optimization, collaborative communication, green communications technologies, machine-to-machine communication, and small cell networks.

Dr. Anpalagan was a recipient of the Dean's Teaching Award in 2011, the Faculty Scholastic, Research and Creativity Award in 2010, and the Faculty Service Award in 2010 at Ryerson University. He has been serving as an Associate Editor for the IEEE COMMUNICATIONS SURVEYS & TUTORIALS since 2012 and *Wireless Personal Communications* (Springer) since 2009, has served as an Associate Editor for IEEE COMMUNICATIONS LETTERS from 2010 to 2013, and a Past Editor for the *EURASIP Journal of Wireless Communications and Networking* from 2004 to 2009. He also served as a Guest Editor for special issues in ACM/Springer *MONET Green Cognitive and Cooperative Communication and Networking* in 2012, *EURASIP Radio Resource Management in 3G+ Systems* in 2006, and *EURASIP Fairness in Radio Resource Management for Wireless Networks* in 2008. He held various positions within IEEE Canada, including the Chair of IEEE Central Canada since 2013, a member of the IEEE Canada Professional Activities Committee from 2009 to 2011, the IEEE Toronto Section Chair from 2006 to 2007, and the ComSoc Toronto Chapter Chair from 2004 to 2005. He is a registered Professional Engineer in the Province of Ontario, Canada.